

TACHOCLINE CONFINEMENT BY AN OSCILLATORY MAGNETIC FIELD

E. Forgács-Dajka and K. Petrovay

Eötvös University, Dept. of Astronomy, Budapest, Pf. 32, H-1518 Hungary

Solar Physics, vol. 203, p. 195-210

Abstract. Helioseismic measurements indicate that the solar tachocline is very thin, its full thickness not exceeding 4% of the solar radius. The mechanism that inhibits differential rotation to propagate from the convective zone to deeper into the radiative zone is not known, though several propositions have been made. In this paper we demonstrate by numerical models and analytic estimates that the tachocline can be confined to its observed thickness by a poloidal magnetic field B_p of about one kilogauss, penetrating below the convective zone and oscillating with a period of 22 years, if the tachocline region is turbulent with a diffusivity of $\eta \sim 10^{10}$ cm²/s (for a turbulent magnetic Prandtl number of unity). We also show that a similar confinement may be produced for other pairs of the parameter values (B_p , η). The assumption of the dynamo field penetrating into the tachocline is consistent whenever $\eta \gtrsim 10^9$ cm²/s.

Keywords: Sun: interior, MHD, tachocline

1. Introduction

Helioseismic inversions of the solar internal rotation during the past decade invariably showed that the surface-like latitudinal differential rotation, pervading the convective zone, changes to a near-rigid rotation in the radiative zone. The change takes place in a very thin layer known as the tachocline (e.g. Kosovichev, 1996). Known properties of the tachocline were recently reviewed by Corbard *et al.* (2001). While for a long time only upper limits were available for the thickness of the tachocline, a more exact determination of the thickness was recently made by several groups (Corbard *et al.*, 1998; Corbard *et al.*, 1999; Charbonneau *et al.*, 1999; Basu and Antia, 2001). Their findings can be summarized as follows. Below the equator the tachocline is centered around at $R = 0.691 \pm 0.003$ solar radii, and its full thickness is $w = 0.04 \pm 0.014$ solar radii.¹ Compared with the internal radius of the (adiabatically stratified) convective zone ($r_{\text{bcz}} = 0.71336 \pm 0.00002$),

¹ By “full thickness” here we mean the radial interval over which the horizontal differential rotation is reduced by a factor of 100. Different authors use different definitions of w , which explains most of the variation among various published values. The e -folding height of differential rotation, i.e. the scale height of the tachocline is then $H = w / \ln 100 \lesssim 0.01 R_{\odot}$.



this implies that the tachocline lies directly beneath the convective zone. There seems to be significant evidence for a slightly prolate form of the tachocline ($R = 0.71 \pm 0.003$ solar radii at a latitude of 60°) and marginal evidence for a thicker tachocline at high latitudes ($w = 0.05 \pm 0.005$ solar radii at 60°). This seems to indicate that at higher latitudes up to half of the tachocline lies in the adiabatically stratified convective zone.

A thorough understanding of the physics of the tachocline is crucial for understanding the solar dynamo for several reasons (see Petrovay, 2000). Firstly, the shear due to differential rotation is generally thought to be responsible for the generation of strong toroidal fields from poloidal fields. This shear is undoubtedly far stronger in the tachocline than anywhere else in the Sun. Second, both linear and nonlinear stability analyses of toroidal flux tubes lying at the bottom of the convective zone show that the storage of these tubes for times comparable to the solar cycle is only possible below the unstably stratified part of the convective zone, in a layer that crudely coincides with the tachocline. Indeed, as flux emergence calculations now provide ample evidence that solar active regions originate from the buoyant instability of 10^5 G flux tubes lying in the stably stratified layers below the convective zone proper (Moreno-Insertis, 1994), it is hard to evade the conclusion that strong magnetic fields oscillating with the dynamo period of 22 years *must* be present in (at least part of) the tachocline.

A magnetic field oscillating with a circular frequency $\omega_{\text{cyc}} = 2\pi/P$, $P = 22$ years is known to penetrate a conductive medium only down to a skin depth of

$$H_{\text{skin}} = (2\eta/\omega_{\text{cyc}})^{1/2} \quad (1)$$

(cf. Garaud, 1999). Using a molecular value for the magnetic diffusivity η , this turns out to be very small (order of a few kilometers) in the solar case, apparently suggesting that the oscillating dynamo field cannot penetrate very deep into the tachocline region. Note, however, that in order to store a magnetic flux of order 10^{23} Mx in the form of a toroidal field of 10^5 G in an active belt of width $\sim 10^5$ km, the storage region must clearly have a thickness of at least several megameters. (Or possibly more, taking into account the strong magnetic flux loss from emerging loops —cf. Petrovay and Moreno-Insertis, 1997; Dorch, private communication.) This is only compatible with equation (1) for $\eta \gtrsim 10^9$ cm²/s.

A turbulent magnetic diffusivity of this order of magnitude is not implausible, given our present lack of detailed information about the physical conditions in the tachocline. The value required is still several orders of magnitude below the diffusivity in the solar convective zone ($\sim 10^{13}$ cm²/s). The turbulence responsible for this diffusivity may be

generated either by non-adiabatic overshooting convection or by MHD instabilities of the tachocline itself. Note that several recent analyses have treated the problem of the stability of the tachocline under various approximations (e.g. Gilman and Dikpati, 2000; see review by Gilman, 2000). The results are not conclusive yet, but it is clearly quite possible that, once all relevant (three-dimensional, nonlinear, MHD) effects are taken into account, the tachocline will prove to be unstable and therefore capable of maintaining a certain level of turbulence. Note that the remaining slight inconsistencies between the standard and seismic solar models also seem to indicate some extra (probably turbulent) mixing in the tachocline layer (Gough, 2000). On the other hand, this turbulent diffusivity should not extend below a depth of a few times 10 Mm to avoid an overdepletion of lithium. Such a shallow depth of the turbulent layer is consistent with the seismic constraints on tachocline thickness, quoted above.

These considerations prompt us to consider the structure of a turbulent tachocline pervaded by an oscillatory magnetic field. For simplicity, the poloidal field will be treated as given, in the form of a simple oscillating field of characteristic strength B_p , of dipolar latitude-dependence, penetrating below the convective zone to a shallow depth of about 30 Mm ($0.04 R_\odot$). We will find that the observed tachocline thickness is reproduced for suitable pairs of the parameter values (B_p , η). This effect would offer a straightforward explanation for the thinness of the tachocline. Indeed, this thinness implies a horizontal transfer of angular momentum that is much more effective than the vertical transport. In our model, the horizontal transport is due to Maxwell stresses in the strong oscillatory magnetic field. Alternative mechanisms proposed for the horizontal transport include a strongly horizontally anisotropic turbulence (Spiegel and Zahn, 1992), non-diffusive hydrodynamical momentum fluxes (Forgács-Dajka and Petrovay, 2001) as well as Maxwell stresses due to a weak permanent internal magnetic field in the radiative interior (MacGregor and Charbonneau, 1999; Rüdiger and Kitchatinov, 1997; Garaud, 2001). The plausibility of the processes implied by the hydrodynamical scenarios is, however, dubious. As pointed out by Canuto (1998), the extremely strong horizontal anisotropy necessary to limit the tachocline to within 4% of the solar radius has never been observed in nature or in laboratory, while non-diffusive fluxes also require an unrealistically high amplitude to do the trick. Internal magnetic fields are certainly able to confine a non-turbulent tachocline (and they will probably be needed to explain the lack of *radial* differential rotation in the solar interior anyway). Nevertheless, on basis of the arguments outlined above we feel that the

alternative concept of a turbulent tachocline pervaded and confined by a dynamo-generated field is worth considering.

2. Estimates

Let us first regard the following model problem. Consider a plane parallel layer of incompressible fluid of density ρ , where the viscosity ν and the magnetic diffusivity η are taken to be constant. At $z = 0$ where z is the vertical coordinate (corresponding to depth in the solar application we have in mind) a periodic horizontal shearing flow is imposed in the y direction:

$$v_{y0} = v_0 \cos(kx) \quad (2)$$

(so that x will correspond to heliographic latitude, while y to the longitude). We assume a two-dimensional flow pattern ($\partial_y = 0$) and $v_x = v_z = 0$ (no “meridional flow”). An oscillatory horizontal “poloidal” field is prescribed in the x direction as

$$B_x = B_p \cos(\omega t) \quad (3)$$

The evolution of the azimuthal components of the velocity and the magnetic field is then described by the corresponding components of the equations of motion and induction, respectively. Introducing $v = v_y$ and using Alfvén speed units for the magnetic field

$$V_p = B_p(4\pi\rho)^{-1/2} \quad b = B_y(4\pi\rho)^{-1/2}, \quad (4)$$

these can be written as

$$\partial_t v = V_p \cos(\omega t) \partial_x b - \nu \nabla^2 v \quad (5)$$

$$\partial_t b = V_p \cos(\omega t) \partial_x v - \eta \nabla^2 b \quad (6)$$

Solutions may be sought in the form

$$v = \bar{v}(x, z) + v'(x, z) f(\omega t) \quad (7)$$

$$b = b'(x, z) f(\omega t + \phi) \quad (8)$$

where f is a 2π -periodic function of zero mean and of amplitude $\mathcal{O}(1)$. (\bar{a} denotes time average of a , while $a' \equiv a - \bar{a}$.)

It will be of interest to consider the (temporal) average of equation (5):

$$0 = \overline{V_p \cos(\omega t) f(\omega t + \phi) \partial_x b' - \nu \nabla^2 \bar{v}} \quad (9)$$

Subtracting this from equation (5) yields

$$\partial_t v' = V_p [\cos(\omega t) f(\omega t + \phi)]' \partial_x b' - \nu \nabla^2 v' \quad (10)$$

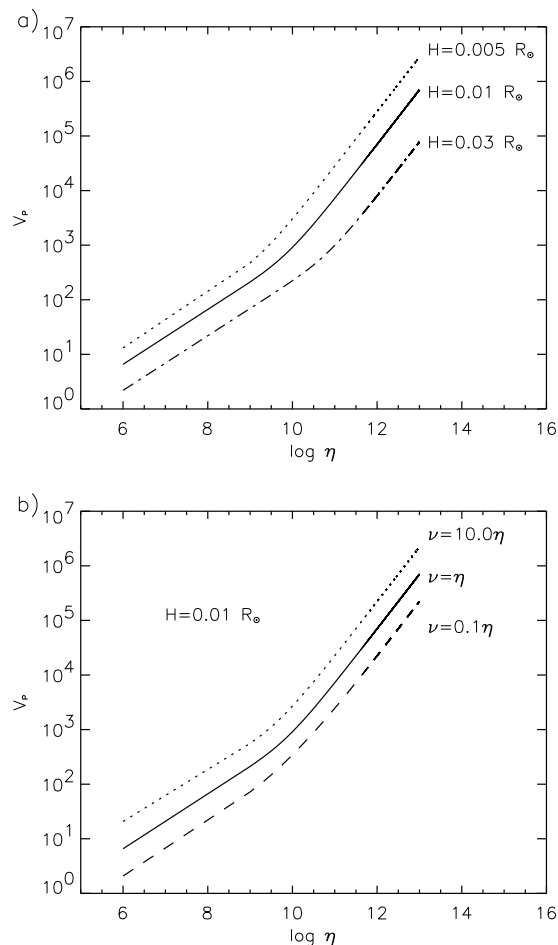


Figure 1. Magnetic field strength in Alfvén speed units V_p necessary to confine the tachocline to thickness H as a function of turbulent magnetic diffusivity η : (a) for $\nu/\eta = 1$ with different values of H ; (b) for $H = 0.01R_\odot$ with different values of the Prandtl number. (Note that, by coincidence, in the solar tachocline $B_p \sim V_p$ to order of magnitude, in CGS units.)

For an estimate, we will suppose $\overline{\cos(\omega t)f(\omega t + \phi)} \in \mathcal{O}(1)$ (i.e. no “conspiracy” between the phases, a rather natural assumption). As $H \ll R$ we may approximate $\nabla^2 \sim H^{-2}$. Estimating the other derivatives as $\partial_t \sim \omega$ and $\partial_x \sim R^{-1}$, (9) yields

$$V_p b' / R \sim \nu \bar{v} / H^2 \quad (11)$$

A similar order-of-magnitude estimate of the terms in equation (10) yields

$$(\omega + \nu / H^2) v' \sim V_p b' / R \quad (12)$$

while from (6) we find in a similar manner

$$\omega b' \sim (V_p + v')V_p/R + \eta b'/H^2 \quad (13)$$

From the last three order-of-magnitude relations one can work out with some algebra

$$V_p^2 = \frac{\nu R^2 \omega (1 + \eta/\omega H^2)(1 + \nu/\omega H^2)}{H^2 (1 + 2\nu/\omega H^2)} \quad (14)$$

Equation (14) then tells us the field amplitude (in Alfvén units) V_p needed to confine the tachocline to a thickness H with given values of the diffusivities and of the oscillation period. If the diffusivities are of turbulent origin one expects $\nu/\eta \simeq 1$ and equation (14) can be used to plot V_p as a function of η for different values of H , with $\omega = 2\pi/22$ yrs (Fig. 1a). Figure 1b illustrates the sensitivity of this result to our assumption about the magnetic Prandtl number ν/η .

Of course, the (V_p, η) pairs that reproduce the observed relation $H \simeq 5$ Mm are also subject to the condition $H \lesssim H_{\text{skin}}$, otherwise the assumption of an oscillatory field pervading the tachocline would not be consistent. Using equation (1), this implies that only the regime $\eta \gtrsim 10^9$ cm²/s should be considered.

Figure 1 thus suggests that an oscillatory poloidal field of about a thousand gauss is able to confine the tachocline to its observed thickness for $\eta \sim 10^{10}$ cm²/s; for higher diffusivities a somewhat stronger field is needed. This figure can then serve as our guide in choosing the parameters of the more realistic spherical models considered in the next section.

3. Numerical Solution

3.1. EQUATIONS

In this section we focus on the numerical solution in the case of spherical geometry, using the realistic solar stratification. The time evolution of the velocity field \mathbf{v} and magnetic field \mathbf{B} are governed by the Navier-Stokes and induction equations:

$$\partial_t \mathbf{v} + (\mathbf{v} \cdot \nabla) \mathbf{v} = -\nabla V - \frac{1}{\rho} \nabla \left(p + \frac{B^2}{8\pi} \right) + \frac{1}{4\pi\rho} (\mathbf{B} \cdot \nabla) \mathbf{B} + \frac{1}{\rho} \nabla \cdot \boldsymbol{\tau}, \quad (15)$$

and

$$\partial_t \mathbf{B} = \nabla \times (\mathbf{v} \times \mathbf{B}) - \nabla \times (\eta \nabla \times \mathbf{B}), \quad (16)$$

where τ is the viscous stress tensor, V is the gravitational potential and p is pressure. These equations are supplemented by the constraints of mass and magnetic flux conservation

$$\nabla \cdot (\rho \mathbf{v}) = 0, \quad (17)$$

$$\nabla \cdot \mathbf{B} = 0. \quad (18)$$

In our model we use the azimuthal component of the equations assuming axial symmetry and we ignore the meridional flow. Then the magnetic and velocity fields can be written as

$$\mathbf{B} = \left[\frac{1}{r^2 \sin \theta} \partial_\theta A, -\frac{1}{r \sin \theta} \partial_r A, B \right], \quad (19)$$

$$\mathbf{v} = r \sin \theta \omega(r, \theta, t) \mathbf{e}_\phi, \quad (20)$$

where the usual spherical coordinates are used, A is the poloidal field potential, B is the toroidal field, ω is the angular velocity and \mathbf{e}_ϕ is the azimuthal unit vector (cf. Rüdiger and Kitchatinov, 1997). In order to present more transparent equations we write the poloidal field potential in the following form:

$$A = a(r, t) \sin^2 \theta. \quad (21)$$

The components of the viscous stress tensor appearing in the azimuthal component of the Navier-Stokes equation are

$$\tau_{\theta\phi} = \tau_{\phi\theta} = \rho\nu \frac{\sin \theta}{r} \partial_\theta \left(\frac{v_\phi}{\sin \theta} \right), \quad (22)$$

$$\tau_{\phi r} = \tau_{r\phi} = \rho\nu r \partial_r \left(\frac{v_\phi}{r} \right), \quad (23)$$

where ν is the viscosity.

Thus, the equations, including the effects of diffusion, toroidal field production by the differential rotation and the Lorentz force, read

$$\begin{aligned} \partial_t \omega = & \left(\partial_r \nu + 4 \frac{\nu}{r} + \frac{\nu}{\rho} \partial_r \rho \right) \partial_r \omega + \nu \partial_r^2 \omega + \frac{3\nu \cos \theta}{r^2 \sin \theta} \partial_\theta \omega + \frac{\nu}{r^2} \partial_\theta^2 \omega \quad (24) \\ & + \frac{a \cos \theta}{2\pi \rho r^3 \sin \theta} \partial_r B - \frac{\partial_r a}{4\pi \rho r^3} \partial_\theta B + \left(\frac{a \cos \theta}{2\pi \rho r^4 \sin \theta} - \frac{\partial_r a \cos \theta}{4\pi \rho r^3 \sin \theta} \right) B, \end{aligned}$$

$$\begin{aligned} \partial_t B = & \frac{2a \sin \theta \cos \theta}{r} \partial_r \omega - \frac{\partial_r a \sin^2 \theta}{r} \partial_\theta \omega \quad (25) \\ & + \left(\frac{2\eta}{r} + \partial_r \eta \right) \partial_r B + \eta \partial_r^2 B + \frac{\eta \cos \theta}{r^2 \sin \theta} \partial_\theta B + \frac{\eta}{r^2} \partial_\theta^2 B \\ & + \left(\frac{\partial_r \eta}{r} - \frac{\eta \cos^2 \theta}{r^2 \sin^2 \theta} - \frac{\eta}{r^2} \right) B. \end{aligned}$$

Under the assumption of no meridional circulation used here, these equations remain unchanged when written in a reference frame rotating with an angular frequency Ω .

3.2. BOUNDARY CONDITIONS

The computational domain for the present calculations consists of just the upper part of the radiative interior, between radii r_{in} and r_{bcz} . We use the same boundary conditions for $\omega(r, \theta, t)$ as those in Elliott (1997). We suppose that the rotation rate at the base of convection zone can be described with the same expression as in the upper part of the convection zone. In accordance with the observations of the GONG network, the following expression is given for Ω_{bcz} :

$$\frac{\Omega_{\text{bcz}}}{2\pi} = 456 - 72 \cos^2 \theta - 42 \cos^4 \theta \text{ nHz.} \quad (26)$$

This is used to give the outer boundary condition on ω ,

$$\Omega + \omega = \Omega_{\text{bcz}} \quad \text{at } r = r_{\text{bcz}}. \quad (27)$$

Ω is chosen as the rotation rate in the radiative interior below the tachocline. On the basis of helioseismic measurements, this value is equal to the rotation rate of the convection zone at a latitude of about 30° , corresponding to $\Omega/2\pi \approx 437$ nHz.

The second boundary condition $\omega = 0$ is imposed at the inner edge of our domain r_{in} .

Our boundary conditions for the toroidal field are simply

$$B = 0 \quad \text{at } r = r_{\text{bcz}} \text{ and } r = r_{\text{in}}. \quad (28)$$

3.3. INITIAL CONDITIONS

The initial conditions chosen for all calculations are

$$\begin{aligned} \omega(r, \theta, t = 0) &= \Omega_{\text{bcz}} - \Omega & \text{at } r = r_{\text{bcz}} \\ \omega(r, \theta, t = 0) &= 0 & \text{at } r < r_{\text{bcz}} \\ B(r, \theta, t = 0) &= 0. \end{aligned} \quad (29)$$

3.4. NUMERICAL METHOD

We used a time relaxation method with a finite difference scheme first order accurate in time to solve the equations. A uniformly spaced grid, with spacings Δr and $\Delta \theta$ is set up with equal numbers of points in the

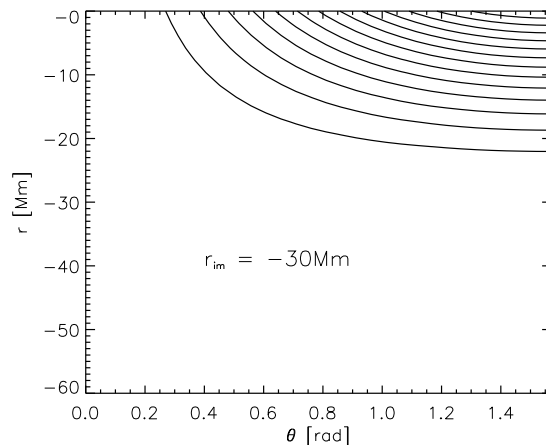


Figure 2. The poloidal field configuration.

r and θ directions. r is chosen to vary from $r_{\text{in}} = 4.2 \times 10^{10}$ cm to r_{bcz} , and θ varies from 0 to $\pi/2$.

The stability of this explicit time evolution scheme is determined by the condition

$$\Delta t < \text{Min} \{ \Delta t_{\text{diff}}, \Delta t_{\text{magdiff}}, \Delta t_{\text{Maxwell}} \} \quad (30)$$

where

$$\Delta t_{\text{diff}} = \frac{\Delta r^2}{2\nu_{\text{max}}} \quad \Delta t_{\text{magdiff}} = \frac{\Delta r^2}{2\eta_{\text{max}}} \quad \Delta t_{\text{Maxwell}} = \left(\frac{\eta}{\nu} \right)^{1/2} \frac{\Delta r}{B_p}. \quad (31)$$

Here, B_p is the amplitude of the poloidal field, defined here as

$$B_p^2 = \text{Max} \left\{ \left| \frac{4a^2}{r_{\text{bcz}}^4} + \frac{(\partial_r a)^2}{r_{\text{bcz}}^2} \right| \right\}. \quad (32)$$

Our calculations are based on a more recent version of the solar model of Guenther *et al.* (1992).

4. Numerical Results and Discussion

In this section we examine the influence of an oscillatory magnetic field on the radial spreading of the differential rotation on the basis of our numerical results. In our calculations the poloidal magnetic field is assumed to be time independent in amplitude, oscillating in time and

a priori known. For the function a of the poloidal field potential the following expression is used:

$$\begin{aligned} a &= A_0 \cos(\omega t) \frac{r_{\text{bcz}}^2}{2} \left(\frac{r - r_{\text{im}}}{r_{\text{bcz}} - r} \right)^2 & r \geq r_{\text{im}} \\ a &= 0 & r_{\text{im}} > r, \end{aligned} \quad (33)$$

where A_0 fixes the field amplitude and r_{im} is the depth of the penetration of the poloidal magnetic field into the radiative interior. As the skin effect should limit the penetration of the oscillatory field below the turbulent tachocline, we set $r_{\text{im}} = 30$ Mm. Figure 2 illustrates the poloidal field geometry. Note that the radial coordinate r shown on the ordinates in our figures has its zero point reset to r_{bcz} , i.e. r in the figures corresponds to $r - r_{\text{bcz}}$. Thus, the negative r values correspond to the layers below the convective zone.

The diffusive timescale over which the solution should relax to a very nearly periodic behaviour is

$$\tau = (r_{\text{bcz}} - r_{\text{in}})^2 / \eta_{\text{min}} \quad (34)$$

where η_{min} is the lowest value of η in the domain, i.e. its value taken at r_{in} . Physically we would expect this value to be close to the molecular viscosity. Using this value in the computations would, however, lead to a prohibitively high number of timesteps to relaxation. (Clearly, the runtime of our computations must be chosen to well exceed τ to reach relaxation.)

Therefore, we first consider the simpler case $\eta = 10^{10}$ cm²/s = const., corresponding to $\tau \sim 120$ years. The results for this case are shown in Figure 3–5 for different amplitudes of the poloidal magnetic field, after relaxation. In accordance with the results of Section 2 it is found that a kilogauss poloidal field (peak amplitude 2400 G) is able to confine the tachocline to its observed thickness.

Figure 6 presents the distribution of the azimuthal component of the Lorentz acceleration

$$f_L = \frac{1}{4\pi\rho} (\mathbf{B} \cdot \nabla) B_\phi \quad (35)$$

in a meridional section of the tachocline, showing polar acceleration and equatorial deceleration. The time variation of the differential rotation and the toroidal magnetic field during a cycle after relaxation is shown in Fig. 7. Note the significant variation with cycle phase.

Finally, in the calculation presented in Figure 8–9 the diffusivity is allowed to vary with radius as

$$\eta = \eta_0 \exp \left(\frac{r - r_{\text{bcz}}}{r_{\text{bcz}} - r_{\text{im}}} \right). \quad (36)$$

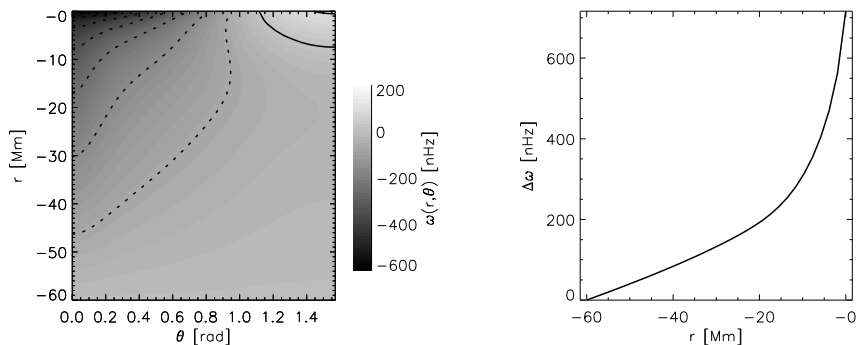


Figure 3. Spreading of the differential rotation into the radiative interior for $B_p = 1603$ G. *Left-hand panel*: contours of the time-average of the angular rotation rate $\omega(r, \theta, t)$ under one dynamo period. Equidistant contour levels are shown, separated by intervals of 100 nHz, starting from 0 towards both non-negative (solid) and negative (dashed) values. *Right-hand panel*: differential rotation amplitude $\Delta\omega$ (defined as the difference of maximal and minimal ω values in a horizontal surface) as a function of radius.

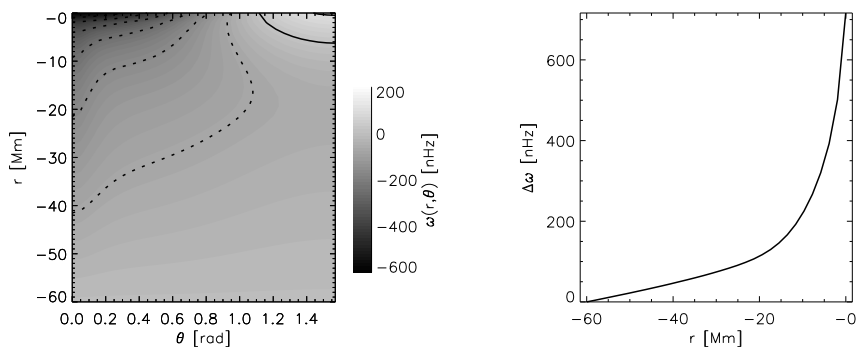


Figure 4. Same as in Figure 3 for $B_p = 2004$ G

This variation, while quantitatively much milder than expected physically, allows us to consider the effects of a variable diffusivity without the necessity of prohibitively long integration times. The influence of the downwards decreasing diffusivity on the solution is found to be small.

Now we turn to the comparison of the detailed spatio-temporal behaviour of our solutions to other models and helioseismic measurements. As a caveat we should stress that, in contrast to the above conclusions about tachocline confinement, these details of our models are unlikely to represent the situation in the real Sun faithfully, as the assumption of a simple dipole geometry (i.e. the use of a “standing wave” instead of a travelling dynamo wave) is clearly not realistic. Yet

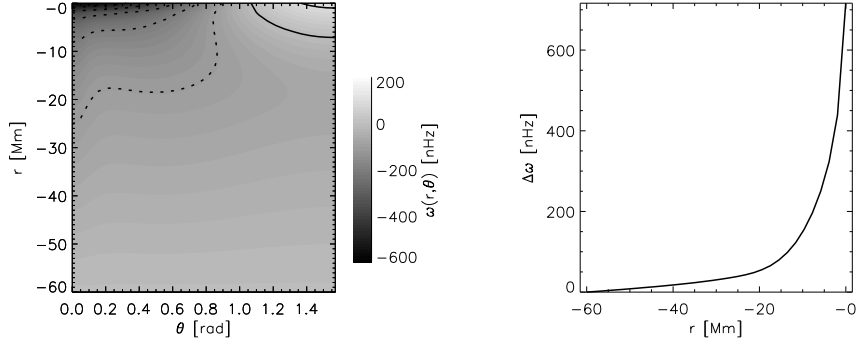


Figure 5. Same as in Figure 3 for $B_p = 2405$ G

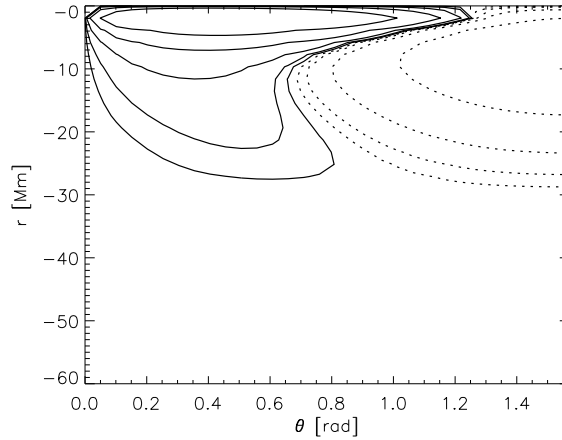


Figure 6. Contours of the time-averaged azimuthal component of the Lorentz acceleration $f_L(r, \theta, t)$ for the case in Fig. 5. Contour levels correspond to $\log |f_L| = (-6, -5.5, -5, -4.5, -4)$, solid contours standing for $f_L > 0$, dashed contours for $f_L < 0$.

it may be interesting from a theoretical point of view to draw some parallels with other work. In particular, the polar “cone” of rotational deceleration discernible in Figs. 3–7 is reminiscent of the similar feature seen in models with a steady internal field (cf. Fig. 2C of MacGregor and Charbonneau, 1999). This feature is, however, likely to disappear or change completely in a model with a poloidal field prescribed as a travelling dynamo wave.

In Fig. 10 we present the time-latitude diagram of angular velocity fluctuations during one cycle. What is remarkable in this plot is not so much the weak poleward migration (which is sensitive to model details, and for other forms of $A(r, \theta, t)$ completely different migration

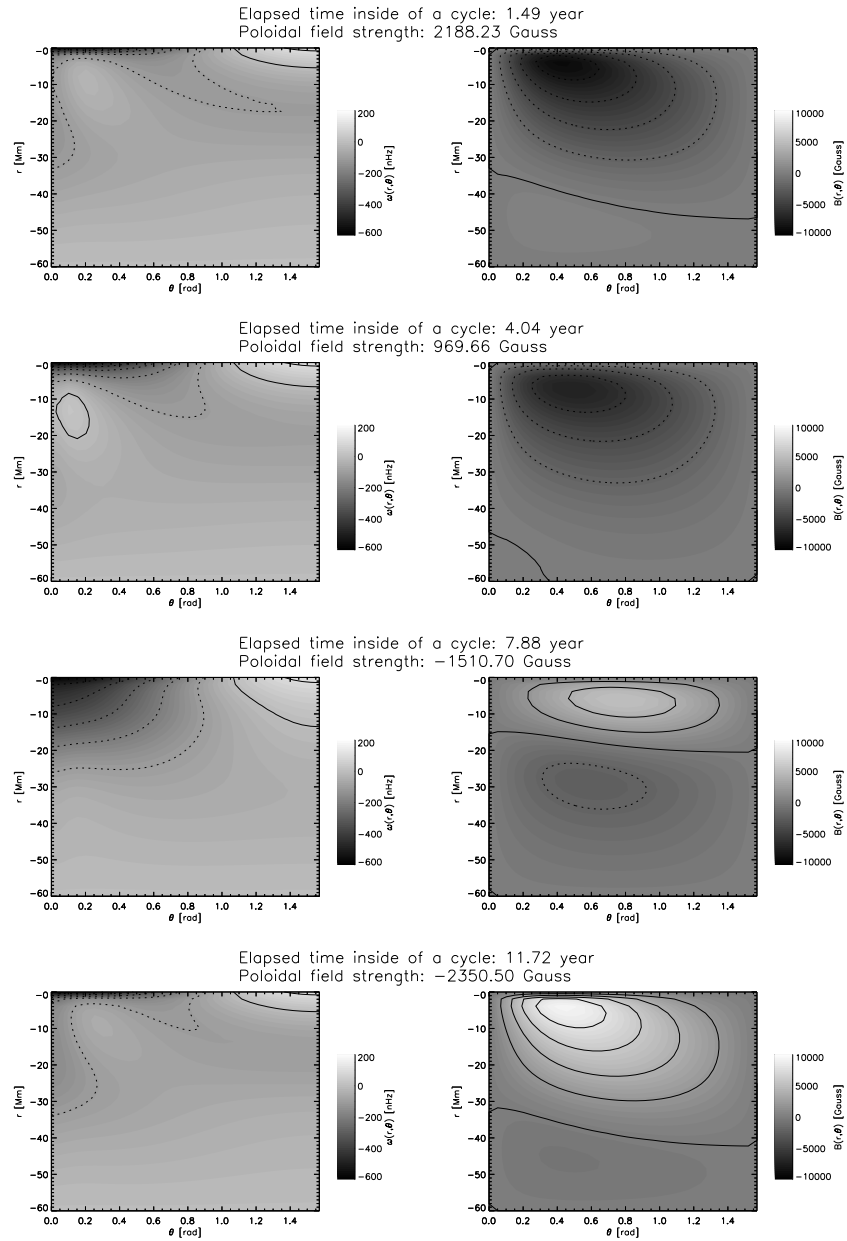


Figure 7. Snapshot of the solution at four cycle phases for $B_p = 2405$ G. $t = 0$ corresponds to poloidal field maximum. *Left-hand panels:* contours of angular rotation rate, as in Fig. 3. *Right-hand panels:* contours of toroidal magnetic field strength. Equidistant contour levels are shown, separated by intervals of 2000 G.

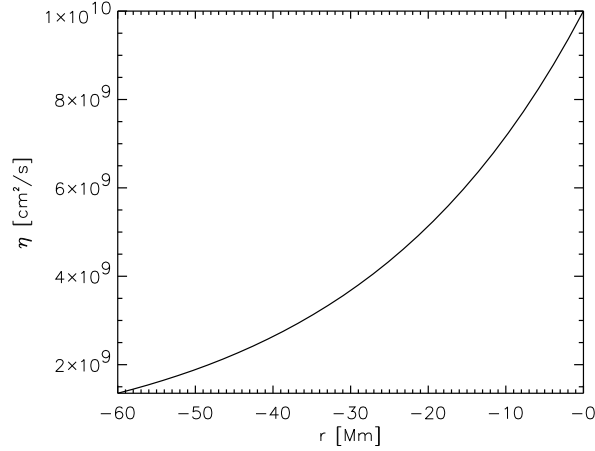


Figure 8. Radial profile of the diffusivity used for Figure 9.

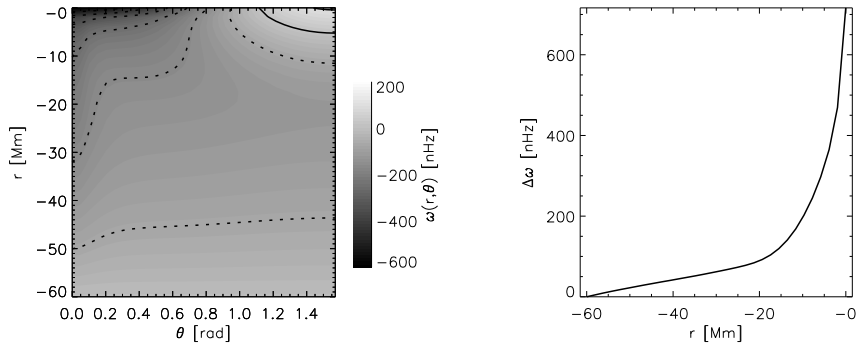


Figure 9. The same as in Figure 5, but the diffusivity is varied in radius.

patterns may result) but the fact that no other periodicity than the imposed 11/22 years is visible. In particular, there is no trace of the controversial 1.3 year periodicity recently claimed by several authors (Corbard *et al.*, 2001 and references therein).

Computer animations of the time evolution illustrated in Fig. 7 and other cases may be found on the accompanying CD-ROM, or they can be downloaded from the following internet address:

<http://astro.elte.hu/kutat/sol/mgconf/mgconfe.html>.

5. Conclusion

We have demonstrated that the tachocline can be confined to its observed thickness by a dipole-like poloidal magnetic field of about one

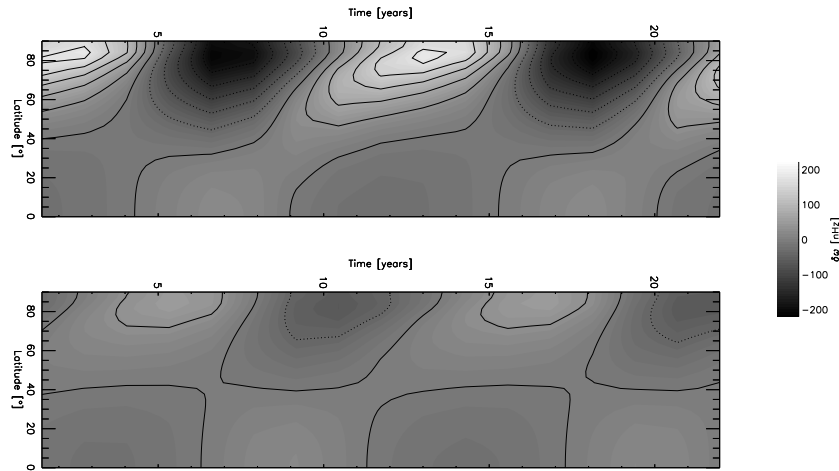


Figure 10. Time–latitude diagram of fluctuations of the angular velocity ω around its temporal average at a given latitude for the case in Fig. 5, at two different levels in the tachocline. *Top*: $r - r_{\text{bcz}} = -3.87$ Mm; *Bottom*: $r - r_{\text{bcz}} = -27.09$ Mm

kilogauss, penetrating below the convective zone and oscillating with a period of 22 years, if the tachocline region is turbulent with a diffusivity of $\eta \sim 10^{10}$ cm²/s. Our estimates presented in Section 2 suggest that a similar confinement may be produced for other pairs of the parameter values (B_p , η). For the numerical computations we assumed a magnetic Prandtl number $\nu/\eta = 1$; Fig. 1(b) gives an impression of the influence of using another ν/η value on the quantitative results

A crucial assumption in these calculations is that the oscillatory poloidal magnetic field does penetrate below the convective zone to depths comparable to the tachocline thickness. This remains an assumption here, the penetration being prescribed a priori by setting the parameter r_{im} . While this should be confirmed later in more general calculations including the evolution equation for the poloidal field, formula (1) does suggest that the assumption is consistent whenever $\eta \gtrsim 10^9$ cm²/s.

This explains the necessity of the high turbulent diffusivity in the tachocline, used in the present models. The high diffusivity, in turn, is the principal reason why the field strength necessary for tachocline confinement is so much higher here than in the case of models with a steady internal remnant magnetic field (MacGregor and Charbonneau, 1999; Rüdiger and Kitchatinov, 1997; Garaud, 2001): as the turbulent magnetic Prandtl number is not expected to differ greatly (i.e. by more than an order of magnitude) from unity, viscous angular momentum transfer is also quite effective.

Another effect that may contribute to the high field strength needed is that here the field is fully anchored in the differentially rotating overlying envelope: since B_r is nonzero at the upper boundary, the magnetic field applies stresses vertically as well as horizontally. In ideal MHD, for a stationary state, magnetic stresses are known to impose $\omega = \text{const.}$ along field lines (Ferraro's theorem). For finite but low diffusivities, field line anchoring can still make a great difference in the resulting rotational profile, as demonstrated by MacGregor and Charbonneau (1999). The fact that periodic oscillations of ω around its temporal mean in our model (Fig. 10) are strongest near the poles, where the field is nearly radial, shows that, despite the high diffusivity, this effect is to some extent also significant in our models. Thus, field line anchoring may be responsible for the fact that the field strengths required in the numerical models exceed somewhat the analytic estimates of Section 2, based on the assumption of a horizontal field.

The ~ 1000 G poloidal field strength assumed here is nonetheless not implausible. Indeed, transport equilibrium models of the poloidal field inside the convective zone (Petrovay and Szakály, 1999) show that the characteristic strength of the poloidal field in the bulk of the convective zone is order of 10 G; flux conservation then sets a lower limit of a few hundred gauss for the poloidal field strength in the region below the convective zone where the field lines close. This is quite compatible with peak values of 1-2000 G.

Our neglect of meridional circulation may also seem worrying to some, given that Spiegel and Zahn (1992) found that the Eddington–Sweet circulation transports angular momentum much more efficiently than viscosity, and so it is the primary mechanism responsible for the inward spreading of the tachocline. This is, however, not expected to be the case for a turbulent tachocline. Owing to the strongly subadiabatic stratification below the convective zone, the timescale of any meridional circulation cannot be shorter than the relevant thermal diffusive timescale (to allow moving fluid elements to get rid of their buoyancy). In the present case the relevant heat conductivity is the turbulent one, so for turbulent Prandtl numbers not very different from unity, the shortest possible timescale for meridional circulation is just comparable to the viscous timescale. Thus, while meridional circulation may possibly indeed have a significant effect on tachocline structure, in our view it is not likely to dominate over turbulent viscosity.

It is clear that the models presented in this paper are still far from being a realistic representation of the solar tachocline. In particular

- In order to limit the number of free parameters, we made no attempt here to simulate the latitudinal migration of the magnetic field during the cycle.

- The diffusivity, if generated by instabilities of the tachocline, should in some way be related to (e.g.) the local shear, instead of being arbitrarily specified.
- The poloidal field evolution should also be consistently calculated in a more complete model.
- Meridional circulation may also be taken into account.

And the list could be continued. Despite these simplifications, we believe that our model convincingly demonstrates the feasibility of tachocline confinement by a dynamo field. Possible generalizations of these models can be made according to the remarks listed above. Work in this direction is in progress.

Acknowledgements

We thank D. B. Guenther for making his solar model available. This work was funded by the OTKA under grants no. T032462 and T034998.

References

- Basu, S. and Antia, H. M.: 2001, in *Helio- and Asteroseismology at the Dawn of the Millennium*, ESA Publ. SP-464, p. 297
- Canuto, V. M.: 1998, *Astrophys. J.* **497**, L51
- Charbonneau, P., Christensen-Dalsgaard, J., Henning, R., Larsen, R. M., Schou, J., Thompson, M. J., and Tomczyk, S.: 1999, *Astrophys. J.* **527**, 445
- Corbard, T., Berthomieu, G., Provost, J., and Morel, P.: 1998, *Astron. Astrophys.* **330**, 1149
- Corbard, T., Blanc-Fraud, L., Berthomieu, G., and Provost, J.: 1999, *Astron. Astrophys.* **344**, 696
- Corbard, T., Jiménez-Reyes, S. J., Tomczyk, S., Dikpati, M., and Gilman, P.: 2001, in *Helio- and Asteroseismology at the Dawn of the Millennium*, ESA Publ. SP-464, p. 265
- Elliott, J. R.: 1997, *Astron. Astrophys.* **327**, 1222
- Forgács-Dajka, E. and Petrovay, K.: 2001, in *Helio- and Asteroseismology at the Dawn of the Millennium*, ESA Publ. SP-464, p. 301
- Garaud, P.: 1999, *Monthly Notices Roy. Astron. Soc.* **304**, 583
- Garaud, P.: 2001, in *Helio- and Asteroseismology at the Dawn of the Millennium*, ESA Publ. SP-464, p. 277
- Gilman, P. A.: 2000, *Solar Phys.* **192**, 27
- Gilman, P. A. and Dikpati, M.: 2000, *Astrophys. J.* **528**, 552
- Gough, D.: 2000, *Solar Phys.* **192**, 3
- Guenther, D. B., Demarque, P., Kim, Y.-C., and Pinsonneault, M. H.: 1992, *Astrophys. J.* **387**, 372
- Kosovichev, A. G.: 1996, *Astrophys. J.* **469**, L61
- MacGregor, K. B. and Charbonneau, P.: 1999, *Astrophys. J.* **519**, 911

- Moreno-Insertis, F.: 1994, in M. Schüssler and W. Schmidt (eds.), *Solar Magnetic Fields*, Proc. Freiburg Internat. Conf., Cambridge UP, p. 117
- Petrovay, K.: 2000, in *The Solar Cycle and Terrestrial Climate*, ESA Publ. SP-463, p. 3
- Petrovay, K. and Moreno-Insertis, F.: 1997, *Astrophys. J.* **485**, 398
- Petrovay, K. and Szakály, G.: 1999, *Solar Phys.* **185**, 1
- Rüdiger, G. and Kitchatinov, L. L.: 1997, *Astr. Nachr.* **318**, 273
- Spiegel, E. A. and Zahn, J.-P.: 1992, *Astron. Astrophys.* **265**, 106

Address for Offprints:

E. Forgács-Dajka
Eötvös University, Dept. of Astronomy
Budapest, Pf. 32, H-1518 Hungary
E-mail: andro@astro.elte.hu

TACHOCLINE CONFINEMENT BY AN OSCILLATORY MAGNETIC FIELD

E. Forgács-Dajka and K. Petrovay

Eötvös University, Dept. of Astronomy, Budapest, Pf. 32, H-1518 Hungary

[*Solar Physics*, submitted (2001)]

Abstract. Helioseismic measurements indicate that the solar tachocline is very thin, its full thickness not exceeding 4% of the solar radius. The mechanism that inhibits differential rotation to propagate from the convective zone to deeper into the radiative zone is not known, though several propositions have been made. In this paper we demonstrate by numerical models and analytic estimates that the tachocline can be confined to its observed thickness by a poloidal magnetic field B_p of about one kilogauss, penetrating below the convective zone and oscillating with a period of 22 years, if the tachocline region is turbulent with a diffusivity of $\eta \sim 10^{10}$ cm²/s (for a turbulent magnetic Prandtl number of unity). We also show that a similar confinement may be produced for other pairs of the parameter values (B_p , η). The assumption of the dynamo field penetrating into the tachocline is consistent whenever $\eta \gtrsim 10^9$ cm²/s.

Keywords: Sun: interior, MHD, tachocline

1. Introduction

Helioseismic inversions of the solar internal rotation during the past decade invariably showed that the surface-like latitudinal differential rotation, pervading the convective zone, changes to a near-rigid rotation in the radiative zone. The change takes place in a very thin layer known as the tachocline (e.g. Kosovichev, 1996). Known properties of the tachocline were recently reviewed by Corbard *et al.* (2001). While for a long time only upper limits were available for the thickness of the tachocline, a more exact determination of the thickness was recently made by several groups (Corbard *et al.*, 1998; Corbard *et al.*, 1999; Charbonneau *et al.*, 1999; Basu and Antia, 2001). Their findings can be summarized as follows. Below the equator the tachocline is centered around at $R = 0.691 \pm 0.003$ solar radii, and its full thickness is $w = 0.04 \pm 0.014$ solar radii.¹ Compared with the internal radius of the (adiabatically stratified) convective zone ($r_{\text{bcz}} = 0.71336 \pm 0.00002$),

¹ By “full thickness” here we mean the radial interval over which the horizontal differential rotation is reduced by a factor of 100. Different authors use different definitions of w , which explains most of the variation among various published values. The e -folding height of differential rotation, i.e. the scale height of the tachocline is then $H = w / \ln 100 \lesssim 0.01 R_{\odot}$.



this implies that the tachocline lies directly beneath the convective zone. There seems to be significant evidence for a slightly prolate form of the tachocline ($R = 0.71 \pm 0.003$ solar radii at a latitude of 60°) and marginal evidence for a thicker tachocline at high latitudes ($w = 0.05 \pm 0.005$ solar radii at 60°). This seems to indicate that at higher latitudes up to half of the tachocline lies in the adiabatically stratified convective zone.

A thorough understanding of the physics of the tachocline is crucial for understanding the solar dynamo for several reasons (see Petrovay, 2000). Firstly, the shear due to differential rotation is generally thought to be responsible for the generation of strong toroidal fields from poloidal fields. This shear is undoubtedly far stronger in the tachocline than anywhere else in the Sun. Second, both linear and nonlinear stability analyses of toroidal flux tubes lying at the bottom of the convective zone show that the storage of these tubes for times comparable to the solar cycle is only possible below the unstably stratified part of the convective zone, in a layer that crudely coincides with the tachocline. Indeed, as flux emergence calculations now provide ample evidence that solar active regions originate from the buoyant instability of 10^5 G flux tubes lying in the stably stratified layers below the convective zone proper (Moreno-Insertis, 1994), it is hard to evade the conclusion that strong magnetic fields oscillating with the dynamo period of 22 years *must* be present in (at least part of) the tachocline.

A magnetic field oscillating with a circular frequency $\omega_{\text{cyc}} = 2\pi/P$, $P = 22$ years is known to penetrate a conductive medium only down to a skin depth of

$$H_{\text{skin}} = (2\eta/\omega_{\text{cyc}})^{1/2} \quad (1)$$

(cf. Garaud, 1999). Using a molecular value for the magnetic diffusivity η , this turns out to be very small (order of a few kilometers) in the solar case, apparently suggesting that the oscillating dynamo field cannot penetrate very deep into the tachocline region. Note, however, that in order to store a magnetic flux of order 10^{23} Mx in the form of a toroidal field of 10^5 G in an active belt of width $\sim 10^5$ km, the storage region must clearly have a thickness of at least several megameters. (Or possibly more, taking into account the strong magnetic flux loss from emerging loops —cf. Petrovay and Moreno-Insertis, 1997; Dorch, private communication.) This is only compatible with equation (1) for $\eta \gtrsim 10^9$ cm²/s.

A turbulent magnetic diffusivity of this order of magnitude is not implausible, given our present lack of detailed information about the physical conditions in the tachocline. The value required is still several orders of magnitude below the diffusivity in the solar convective zone ($\sim 10^{13}$ cm²/s). The turbulence responsible for this diffusivity may be

generated either by non-adiabatic overshooting convection or by MHD instabilities of the tachocline itself. Note that several recent analyses have treated the problem of the stability of the tachocline under various approximations (e.g. Gilman and Dikpati, 2000; see review by Gilman, 2000). The results are not conclusive yet, but it is clearly quite possible that, once all relevant (three-dimensional, nonlinear, MHD) effects are taken into account, the tachocline will prove to be unstable and therefore capable of maintaining a certain level of turbulence. Note that the remaining slight inconsistencies between the standard and seismic solar models also seem to indicate some extra (probably turbulent) mixing in the tachocline layer (Gough, 2000). On the other hand, this turbulent diffusivity should not extend below a depth of a few times 10 Mm to avoid an overdepletion of lithium. Such a shallow depth of the turbulent layer is consistent with the seismic constraints on tachocline thickness, quoted above.

These considerations prompt us to consider the structure of a turbulent tachocline pervaded by an oscillatory magnetic field. For simplicity, the poloidal field will be treated as given, in the form of a simple oscillating field of characteristic strength B_p , of dipolar latitude-dependence, penetrating below the convective zone to a shallow depth of about 30 Mm ($0.04 R_\odot$). We will find that the observed tachocline thickness is reproduced for suitable pairs of the parameter values (B_p , η). This effect would offer a straightforward explanation for the thinness of the tachocline. Indeed, this thinness implies a horizontal transfer of angular momentum that is much more effective than the vertical transport. In our model, the horizontal transport is due to Maxwell stresses in the strong oscillatory magnetic field. Alternative mechanisms proposed for the horizontal transport include a strongly horizontally anisotropic turbulence (Spiegel and Zahn, 1992), non-diffusive hydrodynamical momentum fluxes (Forgács-Dajka and Petrovay, 2001) as well as Maxwell stresses due to a weak permanent internal magnetic field in the radiative interior (MacGregor and Charbonneau, 1999; Rüdiger and Kitchatinov, 1997; Garaud, 2001). The plausibility of the processes implied by the hydrodynamical scenarios is, however, dubious. As pointed out by Canuto (1998), the extremely strong horizontal anisotropy necessary to limit the tachocline to within 4% of the solar radius has never been observed in nature or in laboratory, while non-diffusive fluxes also require an unrealistically high amplitude to do the trick. Internal magnetic fields are certainly able to confine a non-turbulent tachocline (and they will probably be needed to explain the lack of *radial* differential rotation in the solar interior anyway). Nevertheless, on basis of the arguments outlined above we feel that the

alternative concept of a turbulent tachocline pervaded and confined by a dynamo-generated field is worth considering.

2. Estimates

Let us first regard the following model problem. Consider a plane parallel layer of incompressible fluid of density ρ , where the viscosity ν and the magnetic diffusivity η are taken to be constant. At $z = 0$ where z is the vertical coordinate (corresponding to depth in the solar application we have in mind) a periodic horizontal shearing flow is imposed in the y direction:

$$v_{y0} = v_0 \cos(kx) \quad (2)$$

(so that x will correspond to heliographic latitude, while y to the longitude). We assume a two-dimensional flow pattern ($\partial_y = 0$) and $v_x = v_z = 0$ (no “meridional flow”). An oscillatory horizontal “poloidal” field is prescribed in the x direction as

$$B_x = B_p \cos(\omega t) \quad (3)$$

The evolution of the azimuthal components of the velocity and the magnetic field is then described by the corresponding components of the equations of motion and induction, respectively. Introducing $v = v_y$ and using Alfvén speed units for the magnetic field

$$V_p = B_p(4\pi\rho)^{-1/2} \quad b = B_y(4\pi\rho)^{-1/2}, \quad (4)$$

these can be written as

$$\partial_t v = V_p \cos(\omega t) \partial_x b - \nu \nabla^2 v \quad (5)$$

$$\partial_t b = V_p \cos(\omega t) \partial_x v - \eta \nabla^2 b \quad (6)$$

Solutions may be sought in the form

$$v = \bar{v}(x, z) + v'(x, z) f(\omega t) \quad (7)$$

$$b = b'(x, z) f(\omega t + \phi) \quad (8)$$

where f is a 2π -periodic function of zero mean and of amplitude $\mathcal{O}(1)$. (\bar{a} denotes time average of a , while $a' \equiv a - \bar{a}$.)

It will be of interest to consider the (temporal) average of equation (5):

$$0 = \overline{V_p \cos(\omega t) f(\omega t + \phi) \partial_x b' - \nu \nabla^2 \bar{v}} \quad (9)$$

Subtracting this from equation (5) yields

$$\partial_t v' = V_p [\cos(\omega t) f(\omega t + \phi)]' \partial_x b' - \nu \nabla^2 v' \quad (10)$$

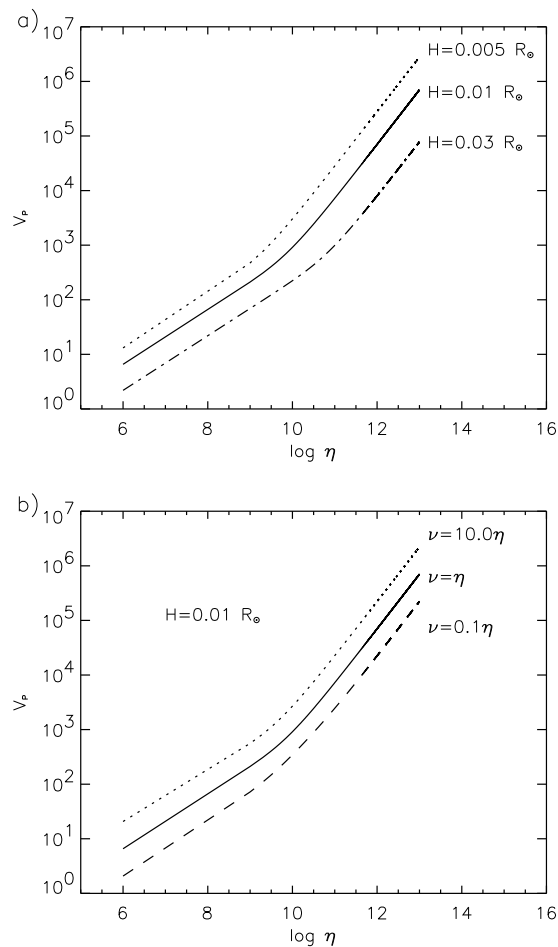


Figure 1. Magnetic field strength in Alfvén speed units V_p necessary to confine the tachocline to thickness H as a function of turbulent magnetic diffusivity η : (a) for $\nu/\eta = 1$ with different values of H ; (b) for $H = 0.01R_\odot$ with different values of the Prandtl number. (Note that, by coincidence, in the solar tachocline $B_p \sim V_p$ to order of magnitude, in CGS units.)

For an estimate, we will suppose $\overline{\cos(\omega t)f(\omega t + \phi)} \in \mathcal{O}(1)$ (i.e. no “conspiracy” between the phases, a rather natural assumption). As $H \ll R$ we may approximate $\nabla^2 \sim H^{-2}$. Estimating the other derivatives as $\partial_t \sim \omega$ and $\partial_x \sim R^{-1}$, (9) yields

$$V_p b' / R \sim \nu \bar{v} / H^2 \quad (11)$$

A similar order-of-magnitude estimate of the terms in equation (10) yields

$$(\omega + \nu / H^2) v' \sim V_p b' / R \quad (12)$$

while from (6) we find in a similar manner

$$\omega b' \sim (V_p + v')V_p/R + \eta b'/H^2 \quad (13)$$

From the last three order-of-magnitude relations one can work out with some algebra

$$V_p^2 = \frac{\nu R^2 \omega (1 + \eta/\omega H^2)(1 + \nu/\omega H^2)}{H^2 (1 + 2\nu/\omega H^2)} \quad (14)$$

Equation (14) then tells us the field amplitude (in Alfvén units) V_p needed to confine the tachocline to a thickness H with given values of the diffusivities and of the oscillation period. If the diffusivities are of turbulent origin one expects $\nu/\eta \simeq 1$ and equation (14) can be used to plot V_p as a function of η for different values of H , with $\omega = 2\pi/22$ yrs (Fig. 1a). Figure 1b illustrates the sensitivity of this result to our assumption about the magnetic Prandtl number ν/η .

Of course, the (V_p, η) pairs that reproduce the observed relation $H \simeq 5$ Mm are also subject to the condition $H \lesssim H_{\text{skin}}$, otherwise the assumption of an oscillatory field pervading the tachocline would not be consistent. Using equation (1), this implies that only the regime $\eta \gtrsim 10^9$ cm²/s should be considered.

Figure 1 thus suggests that an oscillatory poloidal field of about a thousand gauss is able to confine the tachocline to its observed thickness for $\eta \sim 10^{10}$ cm²/s; for higher diffusivities a somewhat stronger field is needed. This figure can then serve as our guide in choosing the parameters of the more realistic spherical models considered in the next section.

3. Numerical Solution

3.1. EQUATIONS

In this section we focus on the numerical solution in the case of spherical geometry, using the realistic solar stratification. The time evolution of the velocity field \mathbf{v} and magnetic field \mathbf{B} are governed by the Navier-Stokes and induction equations:

$$\partial_t \mathbf{v} + (\mathbf{v} \cdot \nabla) \mathbf{v} = -\nabla V - \frac{1}{\rho} \nabla \left(p + \frac{B^2}{8\pi} \right) + \frac{1}{4\pi\rho} (\mathbf{B} \cdot \nabla) \mathbf{B} + \frac{1}{\rho} \nabla \cdot \boldsymbol{\tau}, \quad (15)$$

and

$$\partial_t \mathbf{B} = \nabla \times (\mathbf{v} \times \mathbf{B}) - \nabla \times (\eta \nabla \times \mathbf{B}), \quad (16)$$

where τ is the viscous stress tensor, V is the gravitational potential and p is pressure. These equations are supplemented by the constraints of mass and magnetic flux conservation

$$\nabla \cdot (\rho \mathbf{v}) = 0, \quad (17)$$

$$\nabla \cdot \mathbf{B} = 0. \quad (18)$$

In our model we use the azimuthal component of the equations assuming axial symmetry and we ignore the meridional flow. Then the magnetic and velocity fields can be written as

$$\mathbf{B} = \left[\frac{1}{r^2 \sin \theta} \partial_\theta A, -\frac{1}{r \sin \theta} \partial_r A, B \right], \quad (19)$$

$$\mathbf{v} = r \sin \theta \omega(r, \theta, t) \mathbf{e}_\phi, \quad (20)$$

where the usual spherical coordinates are used, A is the poloidal field potential, B is the toroidal field, ω is the angular velocity and \mathbf{e}_ϕ is the azimuthal unit vector (cf. Rüdiger and Kitchatinov, 1997). In order to present more transparent equations we write the poloidal field potential in the following form:

$$A = a(r, t) \sin^2 \theta. \quad (21)$$

The components of the viscous stress tensor appearing in the azimuthal component of the Navier-Stokes equation are

$$\tau_{\theta\phi} = \tau_{\phi\theta} = \rho\nu \frac{\sin \theta}{r} \partial_\theta \left(\frac{v_\phi}{\sin \theta} \right), \quad (22)$$

$$\tau_{\phi r} = \tau_{r\phi} = \rho\nu r \partial_r \left(\frac{v_\phi}{r} \right), \quad (23)$$

where ν is the viscosity.

Thus, the equations, including the effects of diffusion, toroidal field production by the differential rotation and the Lorentz force, read

$$\begin{aligned} \partial_t \omega = & \left(\partial_r \nu + 4 \frac{\nu}{r} + \frac{\nu}{\rho} \partial_r \rho \right) \partial_r \omega + \nu \partial_r^2 \omega + \frac{3\nu \cos \theta}{r^2 \sin \theta} \partial_\theta \omega + \frac{\nu}{r^2} \partial_\theta^2 \omega \\ & + \frac{a \cos \theta}{2\pi \rho r^3 \sin \theta} \partial_r B - \frac{\partial_r a}{4\pi \rho r^3} \partial_\theta B + \left(\frac{a \cos \theta}{2\pi \rho r^4 \sin \theta} - \frac{\partial_r a \cos \theta}{4\pi \rho r^3 \sin \theta} \right) B, \end{aligned} \quad (24)$$

$$\begin{aligned} \partial_t B = & \frac{2a \sin \theta \cos \theta}{r} \partial_r \omega - \frac{\partial_r a \sin^2 \theta}{r} \partial_\theta \omega \\ & + \left(\frac{2\eta}{r} + \partial_r \eta \right) \partial_r B + \eta \partial_r^2 B + \frac{\eta \cos \theta}{r^2 \sin \theta} \partial_\theta B + \frac{\eta}{r^2} \partial_\theta^2 B \\ & + \left(\frac{\partial_r \eta}{r} - \frac{\eta \cos^2 \theta}{r^2 \sin^2 \theta} - \frac{\eta}{r^2} \right) B. \end{aligned} \quad (25)$$

Under the assumption of no meridional circulation used here, these equations remain unchanged when written in a reference frame rotating with an angular frequency Ω .

3.2. BOUNDARY CONDITIONS

The computational domain for the present calculations consists of just the upper part of the radiative interior, between radii r_{in} and r_{bcz} . We use the same boundary conditions for $\omega(r, \theta, t)$ as those in Elliott (1997). We suppose that the rotation rate at the base of convection zone can be described with the same expression as in the upper part of the convection zone. In accordance with the observations of the GONG network, the following expression is given for Ω_{bcz} :

$$\frac{\Omega_{\text{bcz}}}{2\pi} = 456 - 72 \cos^2 \theta - 42 \cos^4 \theta \text{ nHz.} \quad (26)$$

This is used to give the outer boundary condition on ω ,

$$\Omega + \omega = \Omega_{\text{bcz}} \quad \text{at } r = r_{\text{bcz}}. \quad (27)$$

Ω is chosen as the rotation rate in the radiative interior below the tachocline. On the basis of helioseismic measurements, this value is equal to the rotation rate of the convection zone at a latitude of about 30° , corresponding to $\Omega/2\pi \approx 437$ nHz.

The second boundary condition $\omega = 0$ is imposed at the inner edge of our domain r_{in} .

Our boundary conditions for the toroidal field are simply

$$B = 0 \quad \text{at } r = r_{\text{bcz}} \text{ and } r = r_{\text{in}}. \quad (28)$$

3.3. INITIAL CONDITIONS

The initial conditions chosen for all calculations are

$$\begin{aligned} \omega(r, \theta, t = 0) &= \Omega_{\text{bcz}} - \Omega & \text{at } r = r_{\text{bcz}} \\ \omega(r, \theta, t = 0) &= 0 & \text{at } r < r_{\text{bcz}} \\ B(r, \theta, t = 0) &= 0. \end{aligned} \quad (29)$$

3.4. NUMERICAL METHOD

We used a time relaxation method with a finite difference scheme first order accurate in time to solve the equations. A uniformly spaced grid, with spacings Δr and $\Delta \theta$ is set up with equal numbers of points in the

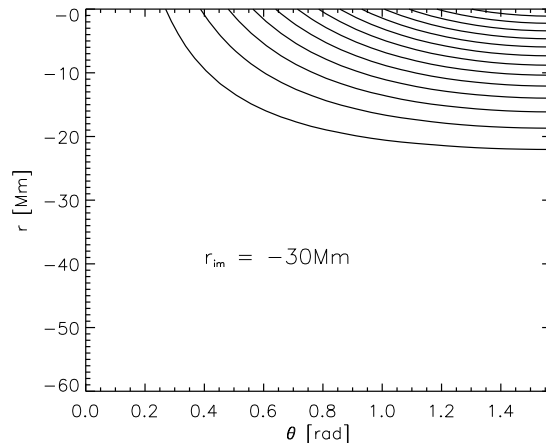


Figure 2. The poloidal field configuration.

r and θ directions. r is chosen to vary from $r_{\text{in}} = 4.2 \times 10^{10}$ cm to r_{bcz} , and θ varies from 0 to $\pi/2$.

The stability of this explicit time evolution scheme is determined by the condition

$$\Delta t < \text{Min} \{ \Delta t_{\text{diff}}, \Delta t_{\text{magdiff}}, \Delta t_{\text{Maxwell}} \} \quad (30)$$

where

$$\Delta t_{\text{diff}} = \frac{\Delta r^2}{2\nu_{\text{max}}} \quad \Delta t_{\text{magdiff}} = \frac{\Delta r^2}{2\eta_{\text{max}}} \quad \Delta t_{\text{Maxwell}} = \left(\frac{\eta}{\nu} \right)^{1/2} \frac{\Delta r}{B_p}. \quad (31)$$

Here, B_p is the amplitude of the poloidal field, defined here as

$$B_p^2 = \text{Max} \left\{ \left| \frac{4a^2}{r_{\text{bcz}}^4} + \frac{(\partial_r a)^2}{r_{\text{bcz}}^2} \right| \right\}. \quad (32)$$

Our calculations are based on a more recent version of the solar model of Guenther *et al.* (1992).

4. Numerical Results and Discussion

In this section we examine the influence of an oscillatory magnetic field on the radial spreading of the differential rotation on the basis of our numerical results. In our calculations the poloidal magnetic field is assumed to be time independent in amplitude, oscillating in time and

a priori known. For the function a of the poloidal field potential the following expression is used:

$$\begin{aligned} a &= A_0 \cos(\omega t) \frac{r_{\text{bcz}}^2}{2} \left(\frac{r - r_{\text{im}}}{r_{\text{bcz}} - r} \right)^2 & r \geq r_{\text{im}} \\ a &= 0 & r_{\text{im}} > r, \end{aligned} \quad (33)$$

where A_0 fixes the field amplitude and r_{im} is the depth of the penetration of the poloidal magnetic field into the radiative interior. As the skin effect should limit the penetration of the oscillatory field below the turbulent tachocline, we set $r_{\text{im}} = 30$ Mm. Figure 2 illustrates the poloidal field geometry. Note that the radial coordinate r shown on the ordinates in our figures has its zero point reset to r_{bcz} , i.e. r in the figures corresponds to $r - r_{\text{bcz}}$. Thus, the negative r values correspond to the layers below the convective zone.

The diffusive timescale over which the solution should relax to a very nearly periodic behaviour is

$$\tau = (r_{\text{bcz}} - r_{\text{in}})^2 / \eta_{\text{min}} \quad (34)$$

where η_{min} is the lowest value of η in the domain, i.e. its value taken at r_{in} . Physically we would expect this value to be close to the molecular viscosity. Using this value in the computations would, however, lead to a prohibitively high number of timesteps to relaxation. (Clearly, the runtime of our computations must be chosen to well exceed τ to reach relaxation.)

Therefore, we first consider the simpler case $\eta = 10^{10}$ cm²/s = const., corresponding to $\tau \sim 120$ years. The results for this case are shown in Figure 3–5 for different amplitudes of the poloidal magnetic field, after relaxation. In accordance with the results of Section 2 it is found that a kilogauss poloidal field (peak amplitude 2400 G) is able to confine the tachocline to its observed thickness.

Figure 6 presents the distribution of the azimuthal component of the Lorentz acceleration

$$f_L = \frac{1}{4\pi\rho} (\mathbf{B} \cdot \nabla) B_\phi \quad (35)$$

in a meridional section of the tachocline, showing polar acceleration and equatorial deceleration. The time variation of the differential rotation and the toroidal magnetic field during a cycle after relaxation is shown in Fig. 7. Note the significant variation with cycle phase.

Finally, in the calculation presented in Figure 8–9 the diffusivity is allowed to vary with radius as

$$\eta = \eta_0 \exp \left(\frac{r - r_{\text{bcz}}}{r_{\text{bcz}} - r_{\text{im}}} \right). \quad (36)$$

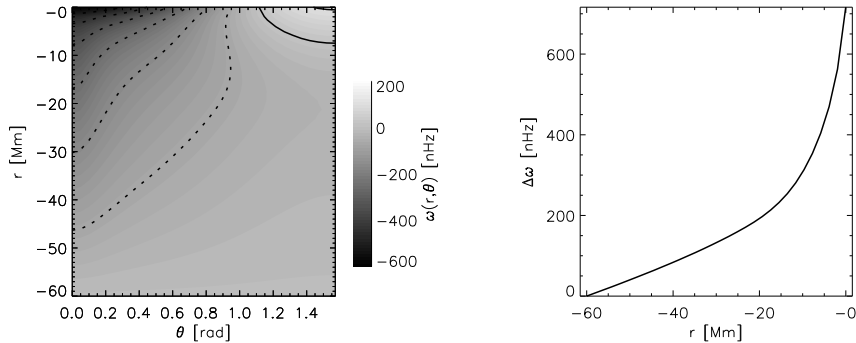


Figure 3. Spreading of the differential rotation into the radiative interior for $B_p = 1603$ G. *Left-hand panel*: contours of the time-average of the angular rotation rate $\omega(r, \theta, t)$ under one dynamo period. Equidistant contour levels are shown, separated by intervals of 100 nHz, starting from 0 towards both non-negative (solid) and negative (dashed) values. *Right-hand panel*: differential rotation amplitude $\Delta\omega$ (defined as the difference of maximal and minimal ω values in a horizontal surface) as a function of radius.

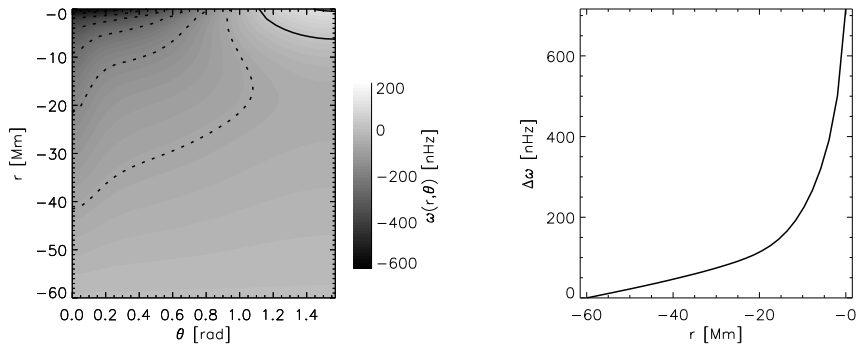


Figure 4. Same as in Figure 3 for $B_p = 2004$ G

This variation, while quantitatively much milder than expected physically, allows us to consider the effects of a variable diffusivity without the necessity of prohibitively long integration times. The influence of the downwards decreasing diffusivity on the solution is found to be small.

Now we turn to the comparison of the detailed spatio-temporal behaviour of our solutions to other models and helioseismic measurements. As a caveat we should stress that, in contrast to the above conclusions about tachocline confinement, these details of our models are unlikely to represent the situation in the real Sun faithfully, as the assumption of a simple dipole geometry (i.e. the use of a “standing wave” instead of a travelling dynamo wave) is clearly not realistic. Yet

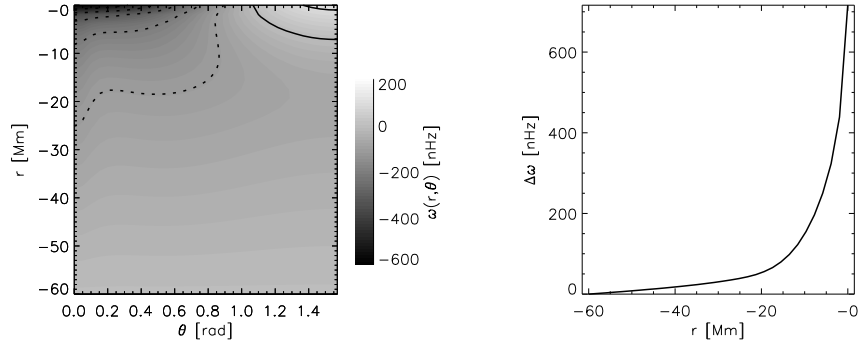


Figure 5. Same as in Figure 3 for $B_p = 2405$ G

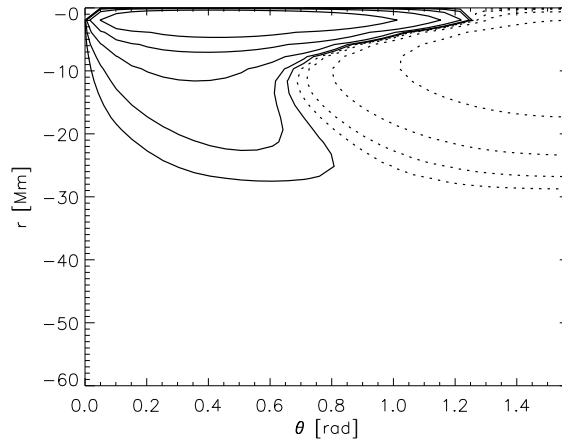


Figure 6. Contours of the time-averaged azimuthal component of the Lorentz acceleration $f_L(r, \theta, t)$ for the case in Fig. 5. Contour levels correspond to $\log |f_L| = (-6, -5.5, -5, -4.5, -4)$, solid contours standing for $f_L > 0$, dashed contours for $f_L < 0$.

it may be interesting from a theoretical point of view to draw some parallels with other work. In particular, the polar “cone” of rotational deceleration discernible in Figs. 3–7 is reminiscent of the similar feature seen in models with a steady internal field (cf. Fig. 2C of MacGregor and Charbonneau, 1999). This feature is, however, likely to disappear or change completely in a model with a poloidal field prescribed as a travelling dynamo wave.

In Fig. 10 we present the time-latitude diagram of angular velocity fluctuations during one cycle. What is remarkable in this plot is not so much the weak poleward migration (which is sensitive to model details, and for other forms of $A(r, \theta, t)$ completely different migration

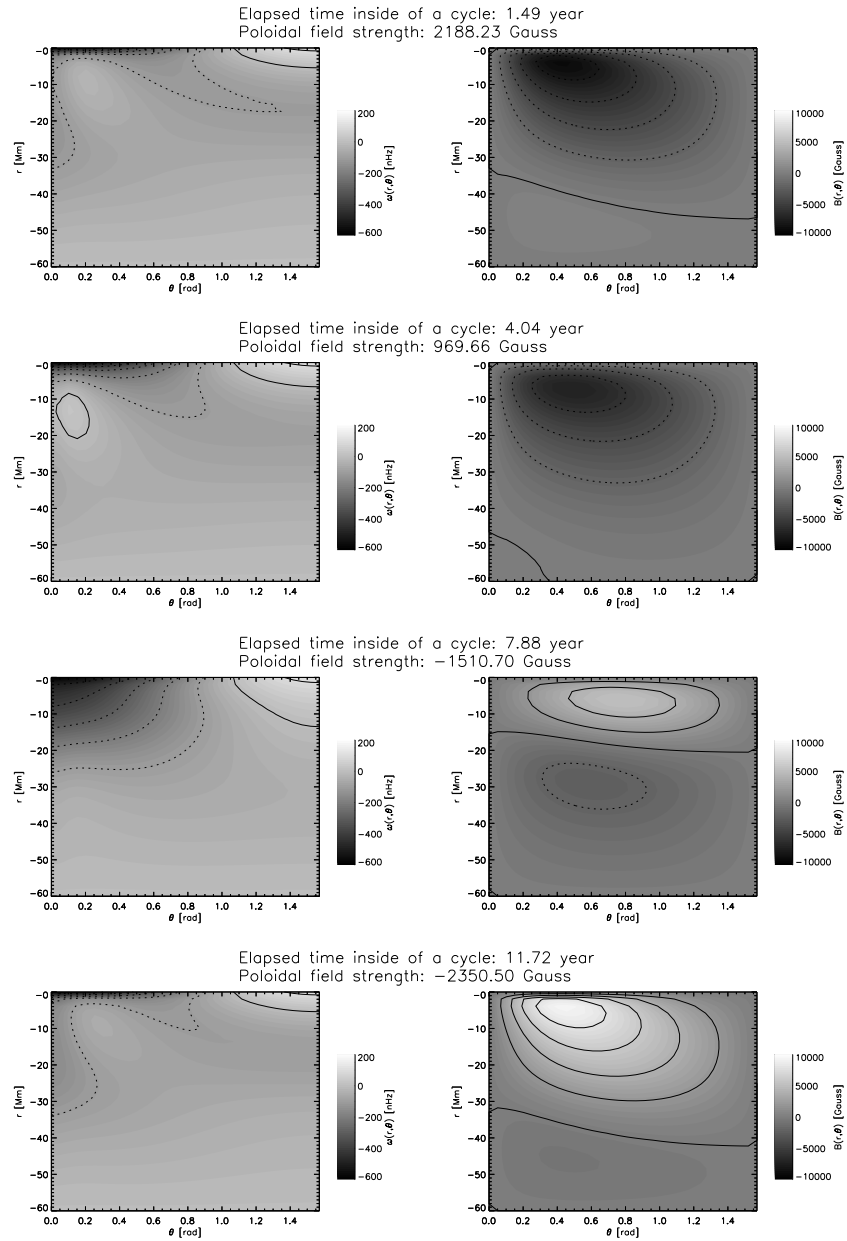


Figure 7. Snapshot of the solution at four cycle phases for $B_p = 2405$ G. $t = 0$ corresponds to poloidal field maximum. *Left-hand panels:* contours of angular rotation rate, as in Fig. 3. *Right-hand panels:* contours of toroidal magnetic field strength. Equidistant contour levels are shown, separated by intervals of 2000 G.

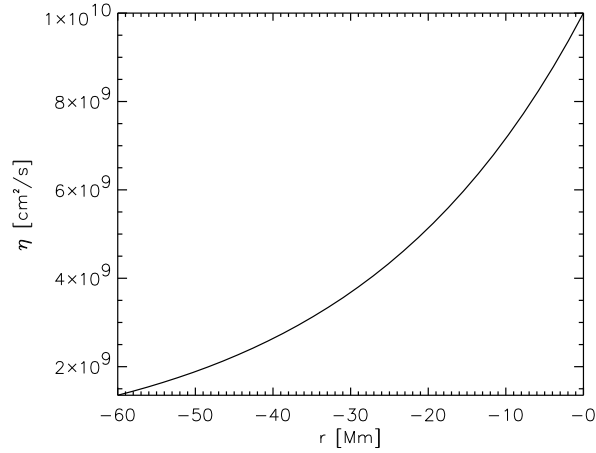


Figure 8. Radial profile of the diffusivity used for Figure 9.

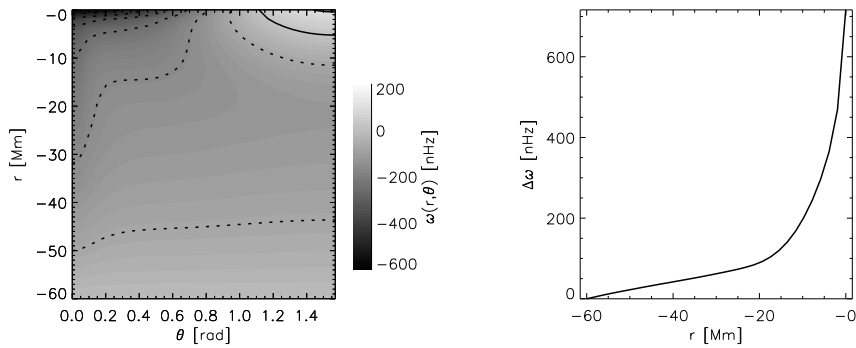


Figure 9. The same as in Figure 5, but the diffusivity is varied in radius.

patterns may result) but the fact that no other periodicity than the imposed 11/22 years is visible. In particular, there is no trace of the controversial 1.3 year periodicity recently claimed by several authors (Corbard *et al.*, 2001 and references therein).

Computer animations of the time evolution illustrated in Fig. 7 and other cases may be found on the accompanying CD-ROM, or they can be downloaded from the following internet address:

<http://astro.elte.hu/kutat/sol/mgconf/mgconfe.html>.

5. Conclusion

We have demonstrated that the tachocline can be confined to its observed thickness by a dipole-like poloidal magnetic field of about one

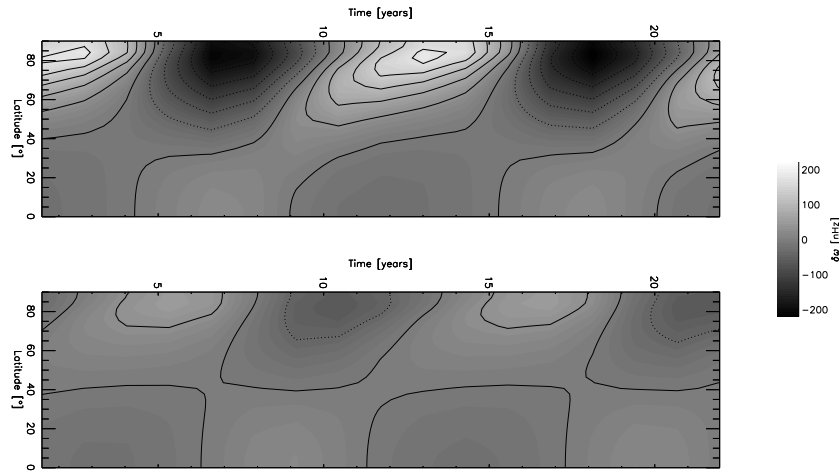


Figure 10. Time–latitude diagram of fluctuations of the angular velocity ω around its temporal average at a given latitude for the case in Fig. 5, at two different levels in the tachocline. *Top*: $r - r_{\text{bcz}} = -3.87$ Mm; *Bottom*: $r - r_{\text{bcz}} = -27.09$ Mm

kilogauss, penetrating below the convective zone and oscillating with a period of 22 years, if the tachocline region is turbulent with a diffusivity of $\eta \sim 10^{10}$ cm²/s. Our estimates presented in Section 2 suggest that a similar confinement may be produced for other pairs of the parameter values (B_p , η). For the numerical computations we assumed a magnetic Prandtl number $\nu/\eta = 1$; Fig. 1(b) gives an impression of the influence of using another ν/η value on the quantitative results

A crucial assumption in these calculations is that the oscillatory poloidal magnetic field does penetrate below the convective zone to depths comparable to the tachocline thickness. This remains an assumption here, the penetration being prescribed a priori by setting the parameter r_{im} . While this should be confirmed later in more general calculations including the evolution equation for the poloidal field, formula (1) does suggest that the assumption is consistent whenever $\eta \gtrsim 10^9$ cm²/s.

This explains the necessity of the high turbulent diffusivity in the tachocline, used in the present models. The high diffusivity, in turn, is the principal reason why the field strength necessary for tachocline confinement is so much higher here than in the case of models with a steady internal remnant magnetic field (MacGregor and Charbonneau, 1999; Rüdiger and Kitchatinov, 1997; Garaud, 2001): as the turbulent magnetic Prandtl number is not expected to differ greatly (i.e. by more than an order of magnitude) from unity, viscous angular momentum transfer is also quite effective.

Another effect that may contribute to the high field strength needed is that here the field is fully anchored in the differentially rotating overlying envelope: since B_r is nonzero at the upper boundary, the magnetic field applies stresses vertically as well as horizontally. In ideal MHD, for a stationary state, magnetic stresses are known to impose $\omega = \text{const.}$ along field lines (Ferraro's theorem). For finite but low diffusivities, field line anchoring can still make a great difference in the resulting rotational profile, as demonstrated by MacGregor and Charbonneau (1999). The fact that periodic oscillations of ω around its temporal mean in our model (Fig. 10) are strongest near the poles, where the field is nearly radial, shows that, despite the high diffusivity, this effect is to some extent also significant in our models. Thus, field line anchoring may be responsible for the fact that the field strengths required in the numerical models exceed somewhat the analytic estimates of Section 2, based on the assumption of a horizontal field.

The ~ 1000 G poloidal field strength assumed here is nonetheless not implausible. Indeed, transport equilibrium models of the poloidal field inside the convective zone (Petrovay and Szakály, 1999) show that the characteristic strength of the poloidal field in the bulk of the convective zone is order of 10 G; flux conservation then sets a lower limit of a few hundred gauss for the poloidal field strength in the region below the convective zone where the field lines close. This is quite compatible with peak values of 1-2000 G.

Our neglect of meridional circulation may also seem worrying to some, given that Spiegel and Zahn (1992) found that the Eddington–Sweet circulation transports angular momentum much more efficiently than viscosity, and so it is the primary mechanism responsible for the inward spreading of the tachocline. This is, however, not expected to be the case for a turbulent tachocline. Owing to the strongly subadiabatic stratification below the convective zone, the timescale of any meridional circulation cannot be shorter than the relevant thermal diffusive timescale (to allow moving fluid elements to get rid of their buoyancy). In the present case the relevant heat conductivity is the turbulent one, so for turbulent Prandtl numbers not very different from unity, the shortest possible timescale for meridional circulation is just comparable to the viscous timescale. Thus, while meridional circulation may possibly indeed have a significant effect on tachocline structure, in our view it is not likely to dominate over turbulent viscosity.

It is clear that the models presented in this paper are still far from being a realistic representation of the solar tachocline. In particular

- In order to limit the number of free parameters, we made no attempt here to simulate the latitudinal migration of the magnetic field during the cycle.

- The diffusivity, if generated by instabilities of the tachocline, should in some way be related to (e.g.) the local shear, instead of being arbitrarily specified.
- The poloidal field evolution should also be consistently calculated in a more complete model.
- Meridional circulation may also be taken into account.

And the list could be continued. Despite these simplifications, we believe that our model convincingly demonstrates the feasibility of tachocline confinement by a dynamo field. Possible generalizations of these models can be made according to the remarks listed above. Work in this direction is in progress.

Acknowledgements

We thank D. B. Guenther for making his solar model available. This work was funded by the OTKA under grants no. T032462 and T034998.

References

- Basu, S. and Antia, H. M.: 2001, in *Helio- and Asteroseismology at the Dawn of the Millennium*, ESA Publ. SP-464, p. 297
- Canuto, V. M.: 1998, *Astrophys. J.* **497**, L51
- Charbonneau, P., Christensen-Dalsgaard, J., Henning, R., Larsen, R. M., Schou, J., Thompson, M. J., and Tomczyk, S.: 1999, *Astrophys. J.* **527**, 445
- Corbard, T., Berthomieu, G., Provost, J., and Morel, P.: 1998, *Astron. Astrophys.* **330**, 1149
- Corbard, T., Blanc-Fraud, L., Berthomieu, G., and Provost, J.: 1999, *Astron. Astrophys.* **344**, 696
- Corbard, T., Jiménez-Reyes, S. J., Tomczyk, S., Dikpati, M., and Gilman, P.: 2001, in *Helio- and Asteroseismology at the Dawn of the Millennium*, ESA Publ. SP-464, p. 265
- Elliott, J. R.: 1997, *Astron. Astrophys.* **327**, 1222
- Forgács-Dajka, E. and Petrovay, K.: 2001, in *Helio- and Asteroseismology at the Dawn of the Millennium*, ESA Publ. SP-464, p. 301
- Garaud, P.: 1999, *Monthly Notices Roy. Astron. Soc.* **304**, 583
- Garaud, P.: 2001, in *Helio- and Asteroseismology at the Dawn of the Millennium*, ESA Publ. SP-464, p. 277
- Gilman, P. A.: 2000, *Solar Phys.* **192**, 27
- Gilman, P. A. and Dikpati, M.: 2000, *Astrophys. J.* **528**, 552
- Gough, D.: 2000, *Solar Phys.* **192**, 3
- Guenther, D. B., Demarque, P., Kim, Y.-C., and Pinsonneault, M. H.: 1992, *Astrophys. J.* **387**, 372
- Kosovichev, A. G.: 1996, *Astrophys. J.* **469**, L61
- MacGregor, K. B. and Charbonneau, P.: 1999, *Astrophys. J.* **519**, 911

- Moreno-Insertis, F.: 1994, in M. Schüssler and W. Schmidt (eds.), *Solar Magnetic Fields*, Proc. Freiburg Internat. Conf., Cambridge UP, p. 117
- Petrovay, K.: 2000, in *The Solar Cycle and Terrestrial Climate*, ESA Publ. SP-463, p. 3
- Petrovay, K. and Moreno-Insertis, F.: 1997, *Astrophys. J.* **485**, 398
- Petrovay, K. and Szakály, G.: 1999, *Solar Phys.* **185**, 1
- Rüdiger, G. and Kitchatinov, L. L.: 1997, *Astr. Nachr.* **318**, 273
- Spiegel, E. A. and Zahn, J.-P.: 1992, *Astron. Astrophys.* **265**, 106

Address for Offprints:

E. Forgács-Dajka
Eötvös University, Dept. of Astronomy
Budapest, Pf. 32, H-1518 Hungary
E-mail: andro@astro.elte.hu